Article

Biological Functions of *Azospirillum brasilense* that can Benefit Host Growth are Responsive to Light Stimuli

Alexandra Bauer Housh[1,2 3], Randi Noel[1,3,4], Avery Powell[1,3,5], Spenser Waller[1,3,5], Stacy L. Wilder[1], Stephanie Sopko[1,6,†], Mary Benoit[1,4], Garren Powell[1,6], Michael J. Schueller[1,2], Richard A. Ferrieri[1,2,3,4,*]

[1.] Missouri Research Reactor Center, University of Missouri, Columbia, MO 65211 (A.B.H., alibauer1109@gmail.com; R.N., rlnhmh@umsystem.edu; A.P., avery.snyder00@gmail.com; S.L.W., wildersl@missouri.edu; S.S., sa207945@atsu.edu; M.B., mvbf4w@mail.missouri.edu; G.P., gmp722@health.missouri.edu; S.W., spenserwaller@gmail.com; M.J.S., schuellerm@missouri.edu; R.A.F., ferrierir@missouri.edu),
[2.] Chemistry Department, University of Missouri, Columbia, MO 65211,
[3.] Interdisciplinary Plant Group, University of Missouri, Columbia, MO 65211,
[4.] Division of Plant Science & Technology, University of Missouri, Columbia, MO 65211,
[5.] School of Natural Resources, University of Missouri, Columbia, MO 65211,
[6.] Department of Biochemistry, University of Missouri, Columbia, MO 65211,
† *Present Address*: Osteopathic School of Medicine, A.T. Still University of Health Sciences, Kirksville, MO 63501, USA.

* *Correspondence*: Richard A. Ferrieri (*Email*: ferrierir@missouri.edu, Tel: 1-573-882-5211)

Abstract: As the use of microbial inoculants in agriculture rises, it becomes important to understand how the environment may influence microbial ability to promote plant growth. This work examines whether there are light dependencies in the biological functions of *Azospirillum brasilense*, a commercialized prolific grass-root colonizer. Though classically defined as non-phototrophic, *A. brasilense* possesses photoreceptors that could perceive light conducted through its host's roots. Evidence for light dependency of four microbial processes were examined and noted: biological nitrogen fixation (BNF), auxin biosynthesis, ATP biosynthesis, and iron and manganese uptake. Functional mutants of *A. brasilense* were leveraged and studied in light and dark environments: HM053 (high BNF and auxin production), *ipdC* (capable of BNF, deficient in auxin production), and FP10 (capable of auxin production, deficient in BNF). HM053 exhibited the highest rate of nitrogenase activity with the greatest light dependency comparing iterations in light and dark environments. The *ipdC* mutant showed similar behavior with relatively lower nitrogenase activity observed, while FP10 did not show a light dependency. Auxin biosynthesis showed strong light dependencies in HM053 and FP10 strains, but not for *ipdC*. Iron is involved in the BNF biological process, and light dependency was observed for microbial $^{59}Fe^{2+}$ uptake in HM053 and *ipdC*, but not FP10. Surprisingly, a light dependency for $^{52}Mn^{2+}$ uptake was only observed in *ipdC*. Finally, ATP biosynthesis was sensitive to light across all three mutants favoring blue light over red light compared to darkness with observed ATP levels in descending order for HM053 > *ipdC* > FP10.

Keywords: *Azospirillum brasilense*, **b**iological nitrogen fixation, microbial auxin biosynthesis, ATP biosynthesis, micronutrient uptake, light stimulation.

1. Introduction

 doi:10.20944/preprints202306.0437.v1

Light has been a vital driver for life on Earth, but it has also proved to be threatening to aerobic organisms due to the photodynamic effect [1]. Over time, organisms have developed adaptations to cope with, or even to exploit, light. It is common knowledge that, as autotrophs, light has vital importance to the growth and development of higher plants. What is less known is how light might impact belowground processes. In a recent study, it was demonstrated that photoreceptors in roots of *Arabidopsis thaliana* could directly perceive certain wavelengths of light (predominantly red light) that was conducted, or "piped", from shoot-to-root tissues where it activated root-expressed phyB, and in turn up-regulated the HY5 transcription factor [2]. HY5 has a role in root growth in response to light, moderating root gravitropism responses [2] and nitrogen uptake [3]. Other examples of light-piping have also been described in bean plants and in maize [4-6]. If plant roots contain photoreceptors and can receive light stimuli through conduction from the aerial portions of the plant, it becomes of interest whether root associating plant growth promoting bacteria (PGPB), can be stimulated by this same light.

Bacteria of the genus *Azospirillum* are Gram-negative, nitrogen fixing bacteria found in the rhizosphere, which are known for their plant growth promoting effects on grasses and cereals worldwide [7-9]. When soil and environmental conditions are ideal, *Azospirillum* can promote plant growth, crop yield, and improve overall nitrogen content within the plant [10-13]. These PGPB are thought to positively impact plant performance due to mechanisms such as their BNF (12) and their ability to produce an important plant developmental hormone, auxin [9, 12, 14-16]. The positive impacts this bacteria has on its host plants has led to the commercialization and use of these bacteria inoculants in certain areas of the world [13, 14, 16, 17].

Like most plants, many microorganisms can be sensitive to light, most notably photosynthetic species such as cyanobacteria, with the most well-studied photoreceptor in photosynthetic bacteria being a phytochrome called bacteriophytochrome [18]. For example, *Rhodospirillum rubrum*, a phototrophic soil microorganism, has been shown to possess photoreceptors that can render its nitrogenase enzyme light sensitive [19]. Photoreceptors, however, are not restricted to phototrophic bacteria. Phytochromes, a family of red/far-red responsive photoreceptors are present in both phototrophic and non-phototrophic microorganisms [1]. *Azospirillum brasilense* contains genes for bacteriophytochrome that control carotenoid-independent responses to photodynamic stress [1]. This indicates that although these bacteria are not phototrophic, they are equipped to sense light and respond to it. Currently, there is little understanding of microbial light-sensing and the impact of light stimuli on microbial biological functions. The early work reporting on photodynamic stress within the Sp7 wild-type strain of *A. brasilense* did not show evidence that light impacted its growth performance [1]. However, a more recent study showed evidence that light stimuli inhibited microbe motility [20]. To our knowledge, this is the first time a light dependency study has been conducted to examine the biological functions of *A. brasilense.*

2. Materials and Methods

2.1. Bacteria Growth

Three functional mutant strains of *Azospirillum brasilense* (HM053, *ipdC,* and FP10) were used in the study and obtained through a material transfer agreement between the Federal University of Paraña (UFPR, Curitiba, PR 174CEP 81531-980, Brazil) and the corresponding author's institution. The HM053 mutant is a natural mutant of the wild-type strain of *A. brasilense* FP2 (Sp7 ATCC 29145 $Nif^{+}Sm^{r}Nal^{r}$) screened through its resistance to ethylenediamine (EDA^{r}) [21, 22]. For the *ipdC* mutant, the indole-3-pyruvate decarboxylase gene (ipdC), coding for a key enzyme of the indole-3-pyruvic acid pathway of auxin (indole-3-acetic acid) biosynthesis in *Azospirillum brasilense,* was functionally disrupted in a site-specific manner using a SacB-cassette insertion into the ipdC gene of wild-type FP2 (Sp7 ATCC 29145) followed by homologous recombination. The method allowed for the

 doi:10.20944/preprints202306.0437.v1

construction of the *ipdC* mutation strain without unwanted sequence changes and relied on the λ Red recombineering method (Direct and Inverted Repeat stimulated excision; DIRex) which works well for generating single point mutations, small insertions or replacements as well as deletions of any size, in a bacterial gene [23]. The resultant knockout strain exhibited a significant reduction in auxin biosynthesis to a level of 10% that of the wild-type strain [15]. The FP10 mutant was obtained by N-nitrosoguanidine mutagenesis of the FP2 wild-type strain of *A. brasilense* and isolated by growth on glutamate medium [24].

The functional mutants were grown in liquid NFbHP-lactate medium following published procedures [12]. The medium contained 20 mM ammonium chloride (NH_4Cl) as a nitrogen source and streptomycin antibiotic (80 μg mL^{-1}). The cultures were grown in a shaking incubator at 30 °C and 130 rpm in 10 mL volume, then re-propagated into 40 mL volume approximately 24-hr prior to starting the tracer administration. The bacteria were grown under two treatment types: 24-hr light and 24-hr dark. During the light experiments, bacteria were propagated directly under a 30 cm x 30 cm red-blue LED light panel intended for indoor plant growth (200 μmol m^{-2} s^{-1} total intensity) that was positioned over the shaking incubator. Lights were left on for the entirety of the bacteria growth period. Dark experiments involved propagation of the bacteria in the dark, handled under indirect light, and grown in the shaking incubator at 30 °C while shielded from any ambient light.

2.2. Plant Growth

Maize kernels from Elk Mound Seed Co. (Hybrid 8100) were dark germinated at room temperature for two days on sterilized paper towels wetted with sterile water in a petri-dish. Seedling's roots were inoculated with isolated bacteria strains suspended in sterile water for 3-hr prior to transplanting to a growth pouch wetted with sterile Hoagland's basal salt solution for approximately one week. They were then transferred to eight-inch plastic cones filled with Turface™ (expanded clay matrix) where the bottom portion of the cone was immersed in de-ionized water. Nutrients were introduced as Hoagland's solution every three days. Growth conditions consisted of 12-hour photoperiods, 500 μmol m^{-2} s^{-1} light intensity, and temperatures of 25 °C/ 20 °C (light/dark) with humidity at 70-80% for two weeks. For BNF studies, roots were removed from the Turface and subjected to the acetylene reduction assay described below for measuring microbial nitrogenase activity. A subset of each root mass collected was also subjcted to drop plate analysis to measure the extent of microbial root inoculation.

2.3. Acetylene Reduction Assay (ARA)

ARAs were conducted to examine functionality of the nitrogenase enzyme under light and dark growth conditions. In this approach, acetylene gas is used to measure nitrogenase activity by its ability to reduce acetylene to ethylene. For details on the ARA see Supplemental Methods.

The bacteria were grown in association with maize roots, which were harvested, weighed (typically ~1 gfw) and placed in a 500-mL mason jar where the top was modified with a gas sampling port to introduce the acetylene gas and withdraw samples later for gas chromatography analysis (Fig. S2). For details on gas chromatography analysis see Supplemental Methods. Ethylene data from this analysis was normalized to CFUs per gram of root tissue as determined by Drop Plate Assays in each experiment. For details on the Drop Plate Assay see Supplemental Methods.

For light sensitivity studies, the mason jars were exposed to full-spectrum white light using a white LED light panel (200 μmol m^{-2} s^{-1} intensity) or individual red LED or blue LED light panels (800 μmol m^{-2} s^{-1} intensities). For full darkness measurements, Mason jars were wrapped in aluminum foil. For consistency, all experimental measurements were carried out at 30 °C.

 doi:10.20944/preprints202306.0437.v1

2.4. Microbial ^{59}Fe Assimilation –

Radioactive $^{59}Fe^{+3}$ and $^{59}Fe^{2+}$ ($t_{1/2}$= 44.5 days) were purchased in 1 mCi doses (equivalent to 37 MBq) from Perkin Elmer Life Sciences (Akron, OH USA). Liquid cultures of bacteria were grown for 24-hr prior to the start of a ^{59}Fe radiotracer study. On the day of an experiment, the cultures were centrifuged, washed with deionized (DI) water, and combined to yield a concentrated pellet of bacteria that was resuspended in 11 mL of DI water. A UV reading was taken at 600 nm ($O.D._{600}$) using a 2 mL aliquot of the 11 mL sample. Of the 9 mL bacteria sample remaining, 9 aliquots of 1 mL were placed into 15-mL labeled Falcon tubes. Dosing with either $^{59}Fe^{3+}$ or $^{59}Fe^{2+}$radiotracers was accomplished by adding 3.6 mL of radiometal diluted in DI water to achieve 20 μCi doses (equivalent to $7.4x10^5$ Bq). Start times were recorded for radioactive decay correction back to common zero times. A 36.0 μL sample of each diluted solution of ^{59}Fe radiotracer was counted in the NaI(Tl) gamma well counter and corrected for volume and detector efficiency back to a value for activity administered to each Falcon tube. Samples were incubated on a Unico TTR-2000 test tube rocker (United Products & Instruments, Inc., Dayton, NJ, USA) for 1, 3, and 5-hr time points either under combined (red/blue) LED lights or wrapped in aluminum foil for dark studies. All radiotracer uptake data was normalized to a standard $O.D._{600}$ value of 2.00.

At each time point, the appropriate samples were centrifuged, washed with water three times, and re-suspended in 1 mL of 1 M HCl. An aliquot (100 μL) of each were removed for activity measurements in the NaI(Tl) gamma well counter for a measure of activity before extraction. The remainder of the washed bacteria were cell-disrupted for 2-min under 100% amplitude to burst cells for ^{59}Fe extraction. Once complete, samples were centrifuged 2-min and the supernatant removed; 100 μL of the supernatant was removed for immediate counting in the NaI(Tl) gamma well detector while the remaining 900 μL was used for iron oxidation state speciation via ion chromatography (Fig. S3). For details on the ion chromatography analysis see Supplemental Methods.

During ion chromatography, the $^{59}Fe^{3+}$ and $^{59}Fe^{2+}$ peaks were collected after separation and the amount of radioactivity in each fraction was measured with the NaI (Tl) gamma well detector. The percent tracer uptake was calculated for each bacterial functional mutant under light and dark conditions at 1, 3 and 5- hour intervals. Additionally, the ratio between $^{59}Fe^{3+}$ and $^{59}Fe^{2+}$was calculated to determine if conversion of the oxidation state of the tracer administered remained the same or was altered by the system or by the bacteria functional mutants.

2.5. Luciferase Chemiluminescence ATP Assay

ATP levels were determined using BacTiter-Glo™ Microbial Cell Viability Assay Reagent (Promega, Madison, WI). This was a luciferase–based assay and the ATP level was determined by measuring luminescence levels compared to ATP standards [25]. Measurement of ATP concentrations within the bacteria cells was performed using a published method of resuspending the bacteria pellet in 500 μL of deionized H_2O and boiling the solution for 10 minutes to break down the cells [26]. For details on the experimental methods see Supplemental Methods. All data was normalized to a standard $O.D._{600}$ value of 2.00.

2.6. Spectrophotometric Auxin Assay

Colorimetric analysis of auxin was performed using Salkowski reagent [27, 28]. When carrying out the assay 200 μL of bacterial culture was mixed with 300 μL of Salkowski reagent and kept in the dark for at least 30-min at room temperature. Additional samples from the same culture were centrifuged where the pellet was separated washed once, resuspended in 500 μL of H_2O and boiled for 10-min to release cellular auxin. 200 μL aliquot was mixed with 300 μL of Salkowski reagent and kept in the dark for at least 30-min at room temperature. Sample absorbances were measured at 536 nm using a

 doi:10.20944/preprints202306.0437.v1

spectrophotometer (Evolution 201 UV/VIS, ThermoFisher Scientific Inc., Waltham, MA, USA). For quantitative analysis, serial dilutions from 0 to 50 mg/L of auxin (Sigma Aldrich, St. Louis, MO, USA) were prepared and used as standards and the bacteria content in all analyses were normalized to a standard $O.D._{600}$ value of 2.00.

2.7. Bacteria ^{52}Mn Assimilation

Radioactive $^{52}Mn^{2+}$ ($t_{½}$ = 5.59 d) decays 29.6% by positron emission. Positron annhilation resulting in two coincident gamma rays at 511 keV energy makes this radioisotope ideal for tracking plant uptake of manganese *via* gamma counting. For these studies, we purchased a 1 mCi dose of $^{52}Mn^{2+}$ (equivalent to 37 MBq) from the University of Wisconsin. Details on how this isotope was produced are found in the Supplemental Methods. Upon receipt of the radioisotope, the dose was pH neutralized since it was shipped in dilute HCl and it was diluted further with DI water for administration to liquid cultures of bacteria isolates following the same procedures described for the ^{59}Fe studies. Samples were incubated on a rocking platform for 1, 3, and 5-hr time points either under LED lights or wrapped in aluminum foil for dark studies.

2.8. Statistical Analysis

Data was subjected to one-way analysis of variance (ANOVA) in R using SigmaPlot 14.5. Tukey's HSD test was used for post hoc correction of comparisons across the treatment conditions (i.e., light vs. dark and red vs. blue light) at a significance level of $P < 0.05$. The $^{59}Fe^{3+/2+}$ and $^{52}Mn^{2+}$ allocation data was also analyzed by Principal Component Analysis (PCA) using XLSTAT software version 2020.3 (Addinsoft Inc., New York, NY 10001, USA).

3. Results and Discussion

3.1. Light Dependencies of BNF and its Supporting Processes in A. brasilense

To investigate whether the activity level of the bacterial nitrogenase enzyme, responsible for BNF capacity, exhibits a light dependency, an ARA was performed with mutant bacteria inoculated maize roots in both full spectrum white light and darkness conditions (Figure 1A-C), as well as in red light and blue light conditions (Figure 1D-E). Regardless of light vs. dark conditions, the ethylene levels slowly increased over the longer root incubation time. This is expected based on natural root emissions of their own ethylene while incubating in the closed jar, as is also measured on non-inoculated maize roots [15]. Natural root ethylene emissions were more obvious with FP10, a non-BNF strain where the slow rise in ethylene over time was due to this process. ARA data was normalized for total root mass in each sample and average microbial content determined from drop plate assays. However, we did not correct for the ethylene contributions derived from natural root emissions because they were miniscule [15] relative to the levels of ethylene generated by the ARA and did not confound interpretation of microbial light dependencies.

Preprints (www.preprints.org) | NOT PEER-REVIEWED | Posted: 6 June 2023 doi:10.20944/preprints202306.0437.v1

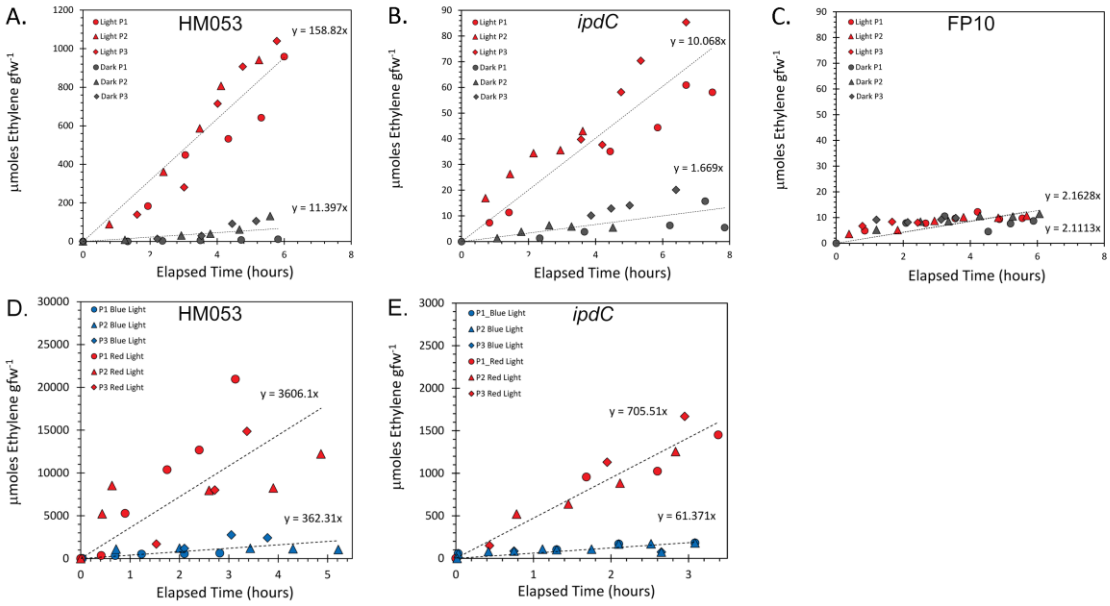

Figure 1. Light dependencies for HM053, *ipdC*, and FP10 strains of *A. brasilense*. Panels A-C represents full spectrum white light (200 µmol m^{-2} s^{-1}) versus darkness data collected from ARAs performed on N=3 plants (labeled P1-P3) that were inoculated with each of the bacteria strains. Panels D&E represent red light versus blue light data collected from ARAs performed on N=3 plants that were inoculated with either HM053 or *ipdC* bacteria. Light intensities for red and blue light studies were 800 µmol m^{-2} s^{-1}, measuring 4-times the intensity of the full spectrum white light.

It is clear from the light/dark ARA studies that the BNF-capable bacteria mutants, HM053 and *ipdC*, showed a significant light dependency in terms of ethylene production indicating that the nitrogenase enzyme in both these strains was more active in the presence of light than in darkness. HM053, which fixes much more nitrogen than *ipdC*, had values much greater than those observed in the latter especially while exposed to light, producing upwards of 1000 µmol ethylene per gram fresh weight of root (µmol ethylene gfw^{-1}) after 6-hr compared to the 90 µmol ethylene gfw^{-1}, respectively. Strikingly, the FP10 mutant, which does not contain an active nitrogenase gene, did not exhibit a light dependency. This seems to point to light sensitivity of the nitrogenase enzyme, or at least the BNF capacity of the bacteria, in *A. brasilense*.

Following the white light studies, comparisons were made between red (660 nm) and blue light (445 nm) stimulation of nitrogenase activity in BNF-capable mutants of HM053 and *ipdC*. Here, it was noted that HM053 and *ipdC* both favored red light for stimulating their nitrogenase enzymes. Additionally, while the wavelength specific light studies were performed at higher light intensities (i.e., 4-times that of the full spectrum white light source) the nitrogenase enzyme in HM053 showed a 6-fold higher level of activity in red light than in the full-spectrum white light after correcting for this intensity difference. On the other hand, blue light stimulation showed approximately the same level of enzyme activity as the full spectrum white light after intensity adjustments were made. Applying the same adjustments for differences in light intensity to the *ipdC* bacteria, we found that red light stimulation boosted nitrogenase activity 17-fold relative to full-spectrum white light, while blue light stimulation resulted in approximately the same level of enzyme activity as the full-spectrum white light.

Light sensitivity in nitrogenase function has been observed in oceanic photosynthetic bacteria, *Crocosphaera watsonii*, in which upon exposure of the bacteria to blue light caused a decrease in nitrogenase activity [30]. In another photosynthetic bacteria species, *Rhodopseudomonas palustris*, a nitrogenase variant exists in which two amino acid substitutions were observed in the FeMo protein allowing the enzyme to reduce CO_2 to CH_4 [31]. In these bacteria, the nitrogenase-variant enzyme was seen to produce methane only in the

Preprints (www.preprints.org) | NOT PEER-REVIEWED | Posted: 6 June 2023 doi:10.20944/preprints202306.0437.v1

presence of light and more methane as the light intensity increased with the limitation that the highest intensity explored was 60 μmol m^{-2} s^{-1} [31]. While light influences on nitrogenase function in non-photosynthetic bacteria have not been explored, light clearly is shown in these instances to influence the BNF capacity of these organisms. *A. brasilense* functional mutants did not exhibit BNF inhibition with exposure to light, as noted for *Crocosphaera watsonii*, suggesting that light influences on BNF activity are perhaps not conserved between photosynthetic and non-photosynthetic bacteria species.

Our interest in ATP biosynthesis as a supporting process is due to BNF being a multi-electron redox process carried out by the nitrogenase enzyme in all diazotrophic species which serves to reduce atmospheric nitrogen to a biologically usable form, NH_3 [32] and is driven by ATP as its chemical energy source. BNF requires at least 16 Mg-ATP molecules to reduce a single dinitrogen molecule [33]. Because nitrogen fixation is so energetically costly, its regulation is essential for balancing BNF with growth performance of any diazotrophic microorganism. Nitrogenase activity is regulated transcriptionally through NifA, the transcriptional activator [9] and post-translationally involving dinitrogenase reductase-activating glycohydrolase together with the P_{II} protein GlnZ [34-36].

Many phototrophic microorganisms such as algae and cyanobacteria carry out photophosphorylation, a light dependent process involving the phosphorylation of ADP making ATP. However, to the best of our knowledge, nothing is known regarding non-phototrophic microorganisms such as *A. brasilense* and whether its ability to biosynthesize ATP is light dependent.

Comparative measurements using the luciferase chemiluminescence assay were conducted in red and blue light conditions using the HM053, *ipdC*, and FP10 mutant strains (Figure 2). All three strains exhibited strong light dependencies in their cellular ATP concentration for both red and blue light when compared to darkness, although in all cases there was a strong preference for blue light. Although *A. brasilense* is non-phototrophic, this observation is consistent with past work demonstrating that blue light was most efficient at promoting photophosphorylation in phototrophic microorganisms [33].

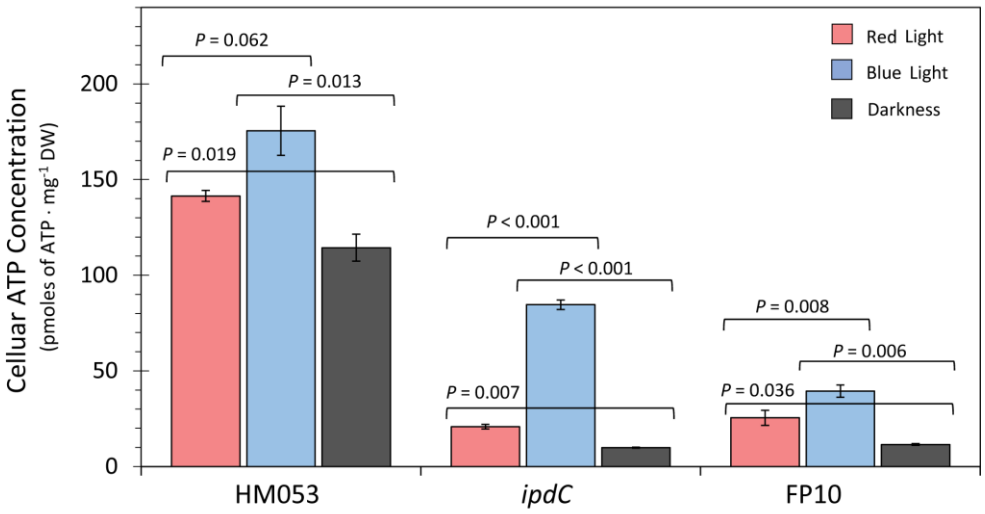

Figure 2. Comparative measurements of cellular ATP concentrations are presented as ρmoles of ATP per mg of dry weight (mg^{-1} DW) of extracted bacteria cells for HM053, *ipdC* and FP10 mutant strains of *A. brasilense* bacteria. Bacteria were grown in liquid cultures at 30 °C for 48-hr. under red light, blue light, and in darkness. Light intensities were 200 μmol m^{-1} s^{-1}. Data bars reflect average values ± SE for N=6 replicates. Levels of significance are shown by the *p*-values where $p < 0.05$ was statistically significant.

Preprints (www.preprints.org) | NOT PEER-REVIEWED | Posted: 6 June 2023 doi:10.20944/preprints202306.0437.v1

Nitrogenase is a two-protein enzyme where one protein contains an iron center and the other an iron-molybdenum center [37]. The iron protein is the only known electron donor to support BNF, thus is vital for its function. The predominant oxidation state of the iron in the nitrogenase iron protein is Fe^{2+} [37].

In the present work, we explored whether microbial iron uptake, as Fe^{3+} and Fe^{2+} exhibited certain light dependencies. Using radioactive ^{59}Fe in its ferric $^{59}Fe^{3+}$ oxidation state, or in its ferrous $^{59}Fe^{2+}$ oxidation state, we were able to measure microbial uptake of tracer over a 5-hr. incubation period as a function of light versus darkness for HM053, *ipdC*, and FP10 mutant strains. As noted earlier, the light studies used a large red/blue light panel that illuminated the entire culture tube rocker assembly with red/blue light of equal intensities. Results in Figure 3A-C show the uptake curves for $^{59}Fe^{3+}$ in the three bacteria strains. Interestingly, HM053 showed a strong light dependency for $^{59}Fe^{3+}$ assimilation where more ferric iron was taken up in darkness than in light. Neither *ipdC*, nor FP10 showed a light dependency for $^{59}Fe^{3+}$ assimilation. Contrary to this, HM053 and *ipdC* showed a light dependency for $^{59}Fe^{2+}$ assimilation where ferrous iron uptake was significantly higher in light than in darkness (Figure 3D & E). This observation correlates well with ARA data in Figure 1, and the fact that Fe^{2+} is vital to the function of the nitrogenase enzyme in the HM053 *and ipdC* strains. However, our HM053 ARA data showed much higher levels of nitrogenase activity than *ipdC*, but the data in Figure 3 indicates that *ipdC* assimilated more $^{59}Fe^{2+}$ over the 5-hr incubation period than HM053. This suggests that Fe^{2+} likely plays other roles in the growth and function of these microorganisms. Also consistent with ARA data FP10, the BNF deficient strain, did not show a light dependency for $^{59}Fe^{2+}$ assimilation (Figure 3F).

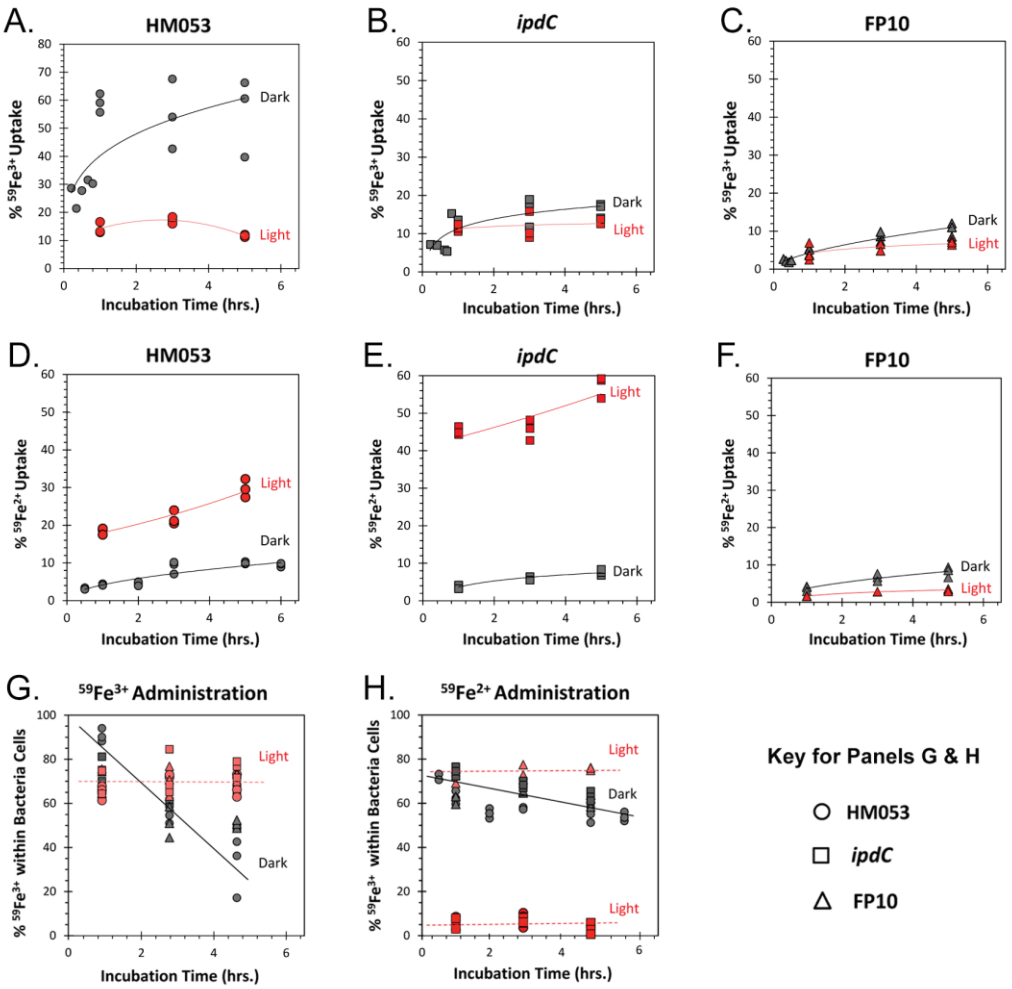

 doi:10.20944/preprints202306.0437.v1

Figure 3. Light dependencies for ^{59}Fe uptake as $^{59}Fe^{3+}$ in HM053, *ipdC* and FP10 bacteria (Panel A-C) and as $^{59}Fe^{2+}$ HM053, *ipdC* and FP10 bacteria (Panel D-F). Studies were conducted in triplicate for each time point measured extending out to 5 hours incubation with radiotracer. Panels G & H also depict how the original oxidation state of the ^{59}Fe tracer may have changed with time once assimilated by the bacteria. Data in Panel G represents the extent of conversion of $^{59}Fe^{3+}$-to-$^{59}Fe^{2+}$ presented as % $^{59}Fe^{3+}$ after administration of $^{59}Fe^{3+}$. Data in Panel H represents the extent of conversion of $^{59}Fe^{2+}$-to-$^{59}Fe^{3+}$ presented as % $^{59}Fe^{3+}$ for continuity after administration of $^{59}Fe^{2+}$.

Lastly, we examined whether there was a light dependency for the conversion between iron oxidation states once the micronutrient was assimilated by the bacteria cell in one or the other oxidation states (Figure 3G & H). Under illumination, all three mutant strains of *A. brasilense* converted a small but consistent 30% of the assimilated $^{59}Fe^{3+}$-to-$^{59}Fe^{2+}$ over the course of the 5-hr incubation period. In contrast, when all three strains were kept in darkness, we observed a linear rise in $^{59}Fe^{3+}$-to-$^{59}Fe^{2+}$ conversion with time which dropped from 90% $^{59}Fe^{3+}$ to 40% $^{59}Fe^{3+}$ over the 5-hr. incubation. A very different story unfolds when $^{59}Fe^{2+}$ was administered. Here, we observed a small, but relatively constant 5% conversion of $^{59}Fe^{2+}$-to-$^{59}Fe^{3+}$ when HM053 or the *ipdC* strains were illuminated, suggesting that their active nitrogenase involved in BNF may rapidly appropriate the assimilated $^{59}Fe^{2+}$ in the iron protein of the enzyme preventing its conversion. When placed in darkness, we found nitrogenase was substantially downregulated as determined by ARA. Under these conditions we expect less $^{59}Fe^{2+}$ to bind to the iron protein and thus more of it remains free to convert to $^{59}Fe^{3+}$. In fact, at the shortest 30-min timepoint, we observed 70% conversion $^{59}Fe^{2+}$-to-$^{59}Fe^{3+}$. Supporting this theory, studies using FP10, the BNF deficient mutant, showed a consistent level of 75% $^{59}Fe^{2+}$-to-$^{59}Fe^{3+}$ conversion over time under illumination. Like the systematic trend observed in darkness when $^{59}Fe^{3+}$ tracer was administered, there was a linear change in $^{59}Fe^{2+}$-to-$^{59}Fe^{3+}$ conversion with time when $^{59}Fe^{2+}$ was administered to bacteria which rose from 30% $^{59}Fe^{2+}$ to 40% $^{59}Fe^{2+}$ over the 5-hr incubation period. We note that regardless of the initial oxidation state of the ^{59}Fe radiotracer administered, when in darkness all bacteria strains appeared to convert a large portion of that tracer to $^{59}Fe^{2+}$ over time.

3.2. Light Dependencies of Auxin Biosynthesis and its Supporting Processes in A. brasilense

One of the best attributes of *A. brasilense* as an agricultural inoculant lies in its ability to biosynthesize the plant relevant hormone auxin [12, 15]. Auxin is best known for its diverse roles in regulating developmental and cellular processes of higher plants impacting axis formation and patterning during post-embryogenesis, vascular elongation, leaf expansion, inflorescence, tropism, and apical dominance [38]. It is also especially important in regulating root development [39, 40], where it can cause extensive lateral root patterning and root hair formation. Because of its diverse nature in regulating host growth and development, light dependency on auxin biosynthesis by the *A. brasilense* microorganism was of interest. Using a spectrophotometric assay, we were able to quantify both the total auxin content contained within the bacteria cells and their liquid growth culture (Figure 4A), as well as isolate the cellular and liquid culture components to calculate cellular auxin excretion as a relative percentage of the total content (Figure 4B).

Preprints (www.preprints.org) | NOT PEER-REVIEWED | Posted: 6 June 2023 doi:10.20944/preprints202306.0437.v1

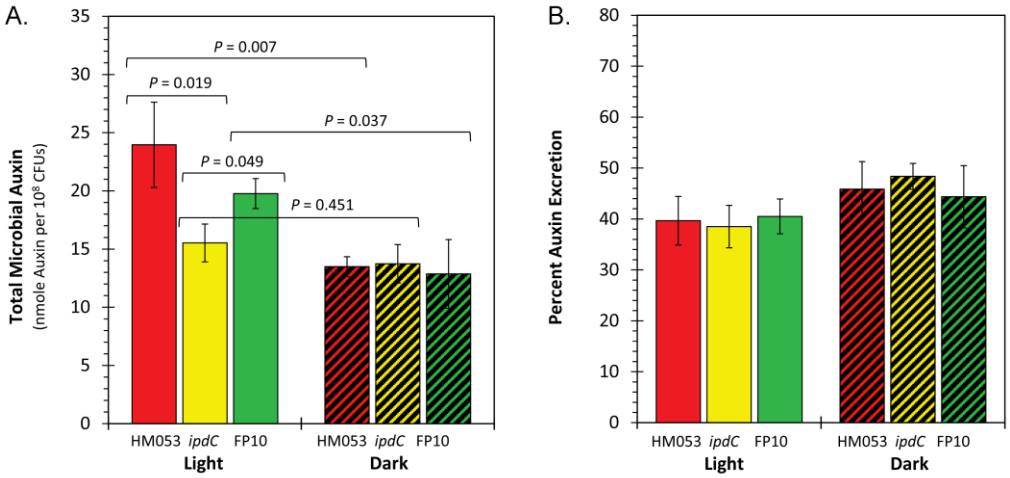

Figure 4. Panel A: total microbial auxin content presented as nmole auxin per 10^8 colony forming units (CFUs). Treatments included light (equal intensities of red and blue light) versus darkness and examined across the functional mutants of *A. brasilense* including HM053, *ipdC* and FP10. Data bars reflect average values ± SE for N=6 replicates. Panel B: relative percent of auxin excreted by the bacteria cells after 48-hr of growth under light treatment.

Like the ^{59}Fe radiotracer assimilation studies, we utilized the same large high intensity red/blue LED light panel to illuminate the liquid culture vials inside the shaking incubator. Our results show that HM053 and FP10 bacteria strains exhibit a significant light dependency when comparing light versus dark condition values. In previous studies, both strains have been reported to biosynthesize auxin at rates of 13.4 ± 0.9 molecules s^{-1} $cell^{-1}$ and 7.0 ± 0.4 molecules s^{-1} $cell^{-1}$, respectively, as determined by our direct radiotracer assay [15], while the *ipdC* auxin deficient mutant strain was estimated to be approximately 10% that of the lower rate. Consistent with earlier findings, the *ipdC* strain did not show a light dependency when comparing the total auxin content between light and dark conditions. Likewise, the relative percent cellular excretion of auxin was the same across all bacterial strains of *A. brasilense* examined and did not appear to change when measurements were conducted in light versus darkness. Thus, we can conclude that the process of microbial cellular auxin excretion is diffusional and likely driven by differences between the physical/chemical properties of the inner cellular and extracellular matrices.

Tryptophan is a key aromatic amino acid precursor in auxin biosynthesis and derives from the shikimate pathway. The shikimate pathway consists of seven sequential enzymatic steps and begins with an aldol-type condensation of two phosphorylated active compounds, the phosphoenolpyruvic acid (PEP), from the glycolytic pathway, and the carbohydrate D-erythrose-4-phosphate, from the pentose phosphate cycle, to give 3-deoxy-D-arabino-heptulosonic acid 7-phosphate (DAHP) (Figure 5).

Preprints (www.preprints.org) | NOT PEER-REVIEWED | Posted: 6 June 2023 doi:10.20944/preprints202306.0437.v1

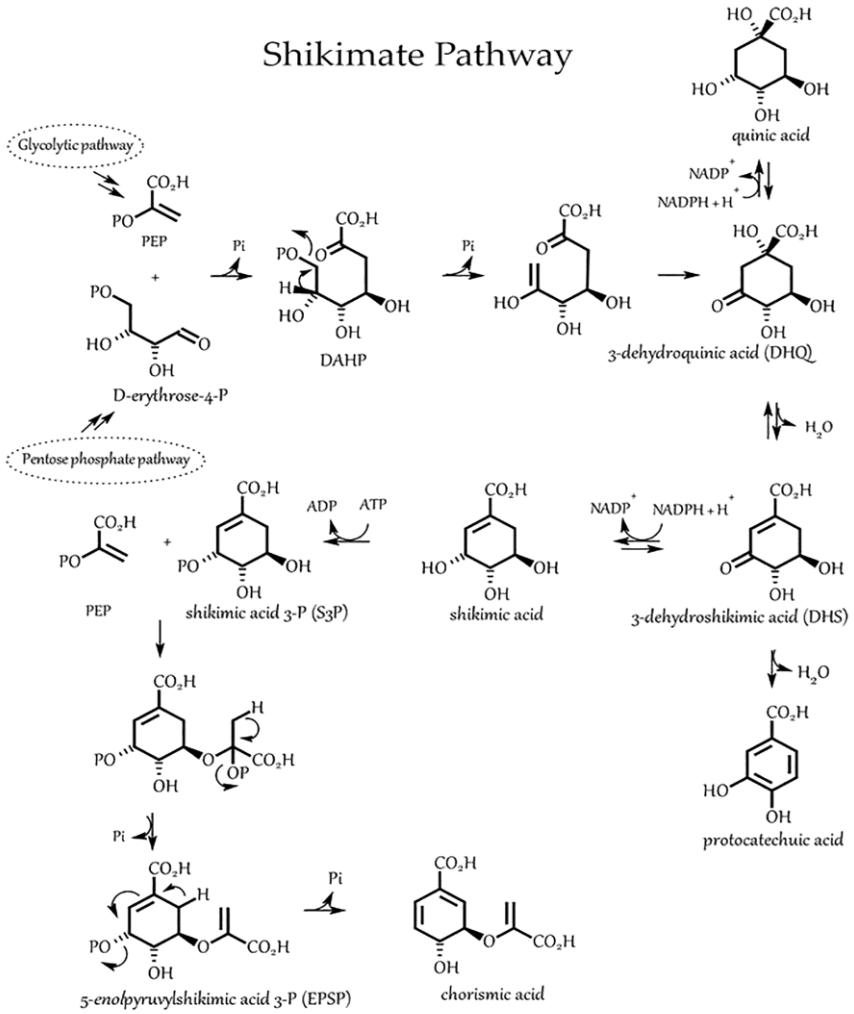

Figure 5. The shikimate pathway common to plants and microorganisms involves seven enzymatic steps that starts with the Aldol condensation of phosphoenol pyruvate (PEP) and erythrose-4-phosphate.

The seven enzymes that catalyze the pathway are known: 3-deoxy-D-arabino-heptulosonate-7-phosphate synthase (DAHPS; EC 4.1.2.15, now EC 2.5.1.54), 3-dehydroquinate synthase (DHQS; EC 4.2.3.4), 3-dehydroquinate dehydratase/shikimate dehydrogenase (DHQ/SDH; EC 4.2.1.10/EC 1.1.1.25), shikimate kinase (SK; EC 2.7.1.71), 5-enolpyruvylshikimate 3-phosphate synthase (EPSPS; EC 2.5.1.19), and chorismate synthase (CS; EC 4.2.3.5). Five of the seven enzymatic steps within the shikimate pathway rely on Mn^{2+} as a cofactor [41, 42]. Hence, a high microbial auxin producing capacity could lend itself to higher turnover of the shikimate pathway with commensurate higher demands for Mn^{2+} and even higher demands for ATP. The latter comes into play in the fifth step of the shikimate pathway. Here the shikimate kinase enzyme catalyzes the phosphorylation of the shikimic acid by ATP producing shikimic acid 3-phosphate and ADP. We've already shown that microbial ATP biosynthesis in *A. brasilense* was light-dependent and was up-regulated across the red and blue light spectrum but favored blue light conditions.

Here, we examined whether the light dependency observed for auxin biosynthesis would manifest in a similar light dependency in microbial Mn^{2+} assimilation. Using radioactive $^{52}Mn^{2+}$ we were able to measure the bacterial assimilation of this micronutrient over time as a function of exposure to light versus darkness using the same functional mutants of *A. brasilense*: HM053, *ipdC*, and FP10 (Figure 6 A-C).

Preprints (www.preprints.org) | NOT PEER-REVIEWED | Posted: 6 June 2023 doi:10.20944/preprints202306.0437.v1

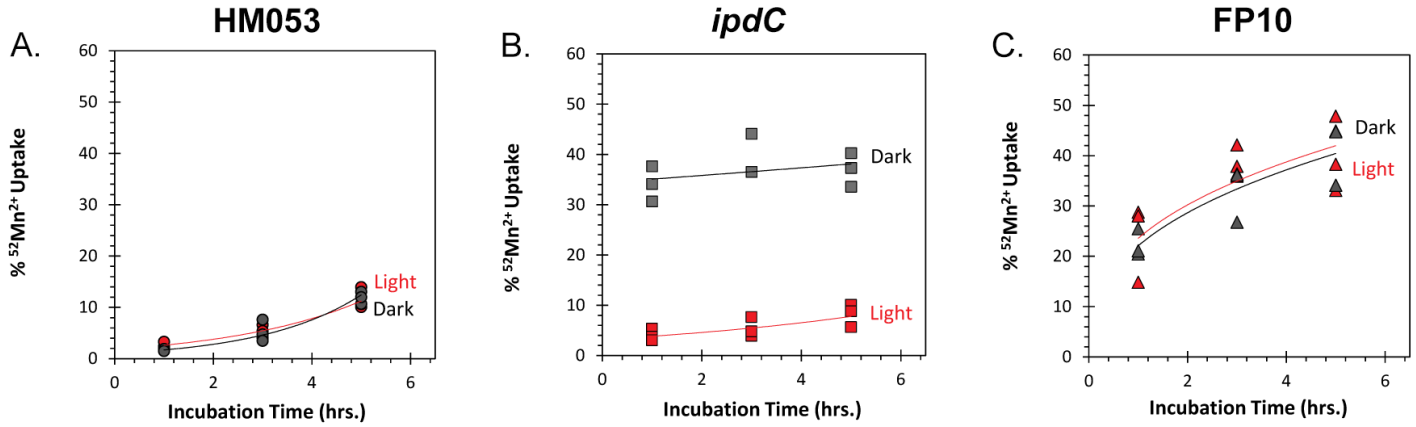

Figure 6. Light dependencies for $^{52}Mn^{2+}$ uptake in HM053, *ipdC*, and FP10 bacteria (Panel A-C). Studies were conducted in triplicate for each time point measured extending out to 5 hours incubation with radiotracer.

Surprisingly, the two high auxin-producing mutants HM053 and FP10 did not show the expected light dependency in their ability to assimilate $^{52}Mn^{2+}$. Consistent with a diffusional micronutrient exchange between the growth matrix and the microbial cell, both mutants showed increased uptake of radiotracer over time. However, FP10, which has a lower rate of auxin biosynthesis than HM053 [15] consistently assimilated more $^{52}Mn^{2+}$ than HM053 over the different incubations timepoints examined. Even more surprisingly, the *ipdC* auxin deficient mutant did exhibit a strong light dependency in its ability to assimilate $^{52}Mn^{2+}$ and assimilated much more $^{52}Mn^{2+}$ in darkness than in light. Altogether, these results strongly suggest that microbial Mn^{2+} demands are not directly aligned with their auxin producing capacity as originally hypothesized. Of course, the role of Mn^{2+} in microbial function likely translates beyond what we described for the shikimate pathway and auxin biosynthesis. More studies are needed to better understand its roles in microbial biology.

Considering that there were interesting light dependencies for $^{59}Fe^{3+}$, $^{59}Fe^{2+}$, and $^{52}Mn^{2+}$ across the different functional mutants of *A. brasilense*, it was of interest to subject the data to Principal Component Analysis across treatment types to elucidate trends (Figure 7 A & B). Here, the information included in our uptake measurements were represented by feature vectors (F1 and F2) representing 56.76% and 43.24% of the information embedded in the $^{59}Fe^{3+}$ and $^{59}Fe^{2+}$ data comparison (Fig. 6A), and 78.29% and 21.71% of the information embedded in the $^{59}Fe^{2+}$ and $^{52}Mn^{2+}$ data comparison (Fig. 6B). Data points from each of the treatment conditions clustered together, indicating behavior within a treatment-type that was similar and distinct from other treatment types. Of greatest note, HM053 mutants in the dark showed elevated uptake of ferric and ferrous radiotracer, indicated by the clustering apart from all other treatments and location toward the end of the ferric feature vector and overall positive Y-value. The auxin-deficient mutant, *ipdC*, also showed greatest ferrous radiotracer uptake but this was not observed until exposed to light; otherwise, the *ipdC* mutant clustered near to the FP10 indicating not much difference, other than a slightly elevated ferric uptake, in iron uptake capacity in the dark relative to FP10 in either light condition. The mutant FP10 in both light and dark were nearly indistinguishable from one another and thus did not change under light stimulus. This demonstrated nicely that the ^{59}Fe uptake capacity of the bacteria correlated with BNF capacity of the mutant strain while also showing a light dependency when BNF capacity was available to the bacteria. Additionally, FP10 showed most similar behavior in comparing ferrous iron and manganese uptake, while *ipdC* showed the most dissimilarity here owing to its significant light dependency noted for $^{52}Mn^{2+}$ uptake.

Preprints (www.preprints.org) | NOT PEER-REVIEWED | Posted: 6 June 2023 doi:10.20944/preprints202306.0437.v1

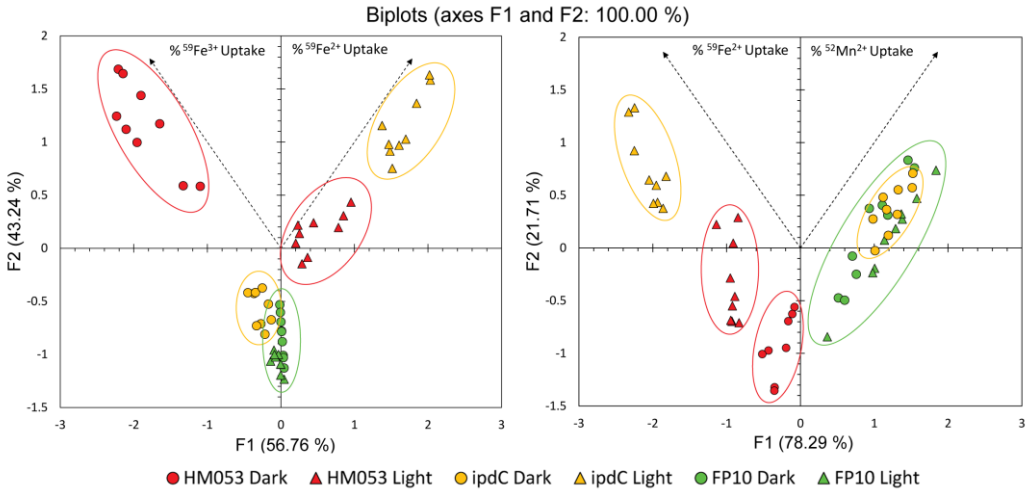

Figure 7. Principle Component Analyses comparing uptake of $^{59}Fe^{3+}$ and $^{59}Fe^{2+}$ (left panel), and $^{59}Fe^{2+}$ and $^{52}Mn^{2+}$ (right panel) as a function of treatment type (light vs. darkness) and microbial type.

4. Conclusions

As the increased implementation of bacterial inoculants for the enhancement of agricultural crop yield and plant nutrition continues, it becomes more important to fully understand the biological functions and mechanisms of action behind their usefulness. Here, we investigated the light dependencies for two important microbial functions associated with plant growth promotion including BNF and auxin biosynthesis. Although not a phototrophic organism, we discovered that both these functions were light sensitive in *A. brasilense* being upregulated in light as opposed to darkness. Additionally, we discovered that certain supporting functions underpinning BNF, and auxin biosynthesis were also light sensitive. Here we found that microbial assimilation of Fe^{2+} as a key element in forming the nitrogen iron protein was light sensitive as was ATP, the major energy source for driving BNF and auxin biosynthesis. Consistent with past studies [1], we found that all three strains of *A. brasilense* showed the same growth performance with each other, and no apparent light dependency. Hence, cellular ATP levels and microbial growth were not directly related. This observation is consistent with past studies in *E. coli* which showed that bacterial growth rates were independent of their cellular ATP concentration [43].

While the present work was not able to connect observed light dependencies of *A. brasilense* with its host's ability to conduct light within the roots, we must wonder why these microorganisms have evolved with traits allowing them to respond to light stimuli. In a time when use of microbial inoculants in agriculture to promote plant growth is becoming a commonplace practice, ways to improve a plant's microbiota might seek to boost plant light transmission belowground or seek to improve the light sensing capabilities of these microorganisms.

Supplementary Materials: Supplemental information is available at www.mdpi.com/xxx/s1 and includes Supplemental Methods and the following Supplemental Figures including: Figure S1, Assembly for preparing batches of acetylene gas for the Acetylene Reduction Assay; Figure S2, Sample collection jar containing maize roots inoculated with *A. brasilense* bacteria; Figure S3, Ion chromatography station used to separate microbial $^{59}Fe^{3+}$ and $^{59}Fe^{2+}$ after radiotracer assimilation; Figure S4, Chemiluminescence spots from the Luciferase Assay using the Typhoon 9000 Imager showing ATP standards and samples done in triplicate for HM053, *ipdC*, and FP10 strains of *A. brasilense* bacteria; and Figure S5, Optical cuvettes showing color differences between HM053, a high auxin producing strain, and *ipdC*, an auxin deficient strain of *A. brasilense* bacteria.

Author Contributions: Experimental design and supervision - R.A.F., M.J.S.; data collection and analysis - A.B.H, R.N, A.P., S.S., S.W. G.P, M.B., S.L.W., initial draft - R.A.F.; final draft - all authors.

Funding: This research was supported by Agriculture and Food Research Initiative Award No. 2017-67013-26216 from the USDA National Institute of Food and Agriculture.

Data Availability Statement: All data needed to evaluate the conclusions in the paper are present in the main text or the supplementary materials.

Acknowledgments: We would like to thank Prof. Emanuel de Souza (U. Paraná, Brazil) whose institution provided the functional mutants of *A. brasilense* in this work.

Conflicts of Interest: The authors declare no conflict of interest.

References

1. Kumar, S., Kateriya, S., Singh, V.S., Tanwar, M., Agarwal, S., Singh, H., Khurana, J. P., Amla, D. V., Tripathi, A. K. Bacteriophytochrome controls carotenoid-independent response to photodynamic stress in a non-photosynthetic rhizobacterium, *Azospirillum brasilense* Sp7. *Scientific Reports.* **2012**, *2(1)*, 872.
2. Lee, H.J., Ha, J.H., Kim, S.G., Choi, H.K., Kim, Z.H., Han, Y.-J., Kim, J.-I., Oh, Y., Fragoso, V., Shin, K., Hyeon, T., Choi, H.-G., Oh, K.-H., Baldwin, I.T., Park, C.-M. Stem-piped light activates phytochrome B to trigger light responses in Arabidopsis thaliana roots. *Sci Signal*. **2016**, *9(452)*, ra106.
3. van Gelderen, K., Kang, C., Pierik, R. Light Signaling, Root Development, and Plasticity. Plant Physiol. 2018; 176(2):1049–60.
4. Kakuszi, A., Sárvári, É., Solti, Á., Czégény, G., Hideg, É., Hunyadi-Gulyás, É., Bóka, K., Böddi, B. Light piping driven photosynthesis in the soil: Low-light adapted active photosynthetic apparatus in the under-soil hypocotyl segments of bean (*Phaseolus vulgaris*). *Journal of Photochemistry and Photobiology B: Biology*. **2016**, *161*, 422–9.
5. Waller, S., Wilder, S.L., Schueller, M.J., Ferrieri, R.A. Plants use the suberin biopolymer to conduct light. *Polymers* **2022**, *14*, 5387.
6. Sun, Q., Yoda, K., Suzuki, H. Internal axial light conduction in the stems and roots of herbaceous plants. *Journal of Experimental Botany*. **2005**, *56(409)*, 191–203.
7. Okon, Y. Azospirillum/Plant Associations. *CRC Press*, Boca Raton, FL, **1993**. 192 p.
8. Okon, Y., Vanderleyden, J. Root-associated *Azospirillum* species can stimulate plants. *ASM News*. **1997**, *63(7)*, 366–70.
9. Steenhoudt, O., Vanderleyden, J. *Azospirillum*, a free-living nitrogen-fixing bacterium closely associated with grasses: genetic, biochemical, and ecological aspects. *FEMS Microbiol Rev*. **2000**, *24(4)*, 487–506.
10. James, E., Baldani, J. The role of biological nitrogen fixation by non-legumes in the sustainable production of food and biofuels. *Plant and Soil***. 2012**, 356, 1–3.
11. Richardson, A., Barea, J., Mcneill, A., Prigent-Combaret, C., Richardson, A.E., Barea J.M., McNeill, A.M., Prigent-Combaret, C. Acquisition of phosphorus and nitrogen in the rhizosphere and plant growth promotion by microorganisms. *Plant and Soil*. **2009,** *321*, 305-339.
12. Pankievicz, V.C.S., do Amaral, F.P., Santos K.F.D.N., Agtuca, B., Xu, Y., Schueller, M.J., Arisi, A.C.M., Steffens, M.B.R., de Souza, E.M., Pedrosa, F.O., Ferrieri, R.A., Stacey, G. Robust biological nitrogen fixation in a model grass–bacterial association. *The Plant Journal*. **2015**, *81(6)*, 907–919.
13. Okon, Y., Labandera-Gonzalez, C.A. Agronomic applications of *Azospirillum*: an evaluation of 20 years worldwide field inoculation. *Soil Biol Biochem*. **1994**, *26(12)*, 1591–601.
14. Pedraza, R.O., Bellone, C.H., Carrizo de Bellone, S., Boa Sorte, P.M.F., Teixeira K. *Azospirillum* inoculation and nitrogen fertilization effect on grain yield and on the diversity of endophytic bacteria in the phyllosphere of rice rainfed crop. European *Journal of Soil Biology*. **2009,** *45(1)*, 36–43.
15. Housh, A.B., Powell, G., Scott, S., Anstaett, A., Gerheart, A., Benoit, M., Waller, S., Powell, A., Guthrie, J.M., Higgins, B., Wilder, S.L., Schueller, M.J., Ferrieri, R.A. Functional mutants of *Azospirillum brasilense* elicit beneficial physiological and metabolic responses in Zea mays contributing to increased host iron assimilation. *The ISME Journal*. **2021**, *15*, 1505–1522.
16. Dobbelaere, S., Croonenborghs, A., Thys, A., Ptacek, D., Vanderleyden, J, Dutto, P., Labandera-Gonzalez, C., Caballero-Mellado, J., Aguirre, J.F., Kapulnik, Y., Brener, S., Burdman, S., Kadouri, D., Sarig, S., Okon, Y. Responses of agronomically important crops to inoculation with Azospirillum. *Functional Plant Biol*. **2001**, *28(9)*, 871–9.
17. Suhameena, B., Devi, S., Gowri, R., Kumar, S.D. Utilization of *Azospirillum* as a biofertilizer – An overview. *International Journal of Pharmaceutical Sciences Review and Research*. **2020**, *62*, 141-145.
18. Giraud, E., Lavergne, J, Verméglio, A. Chapter 9 - Characterization of Bacteriophytochromes from Photosynthetic Bacteria: Histidine Kinase Signaling Triggered by Light and Redox Sensing. *Methods in Enzymology*, **2010**, *471*, 135–159.
19. Carithers, R.P., Yoch, D.C., Arnon, D.I. Two Forms of Nitrogenase from the Photosynthetic Bacterium Rhodospirillum rubrum. *J Bacteriol*. **1979**, *137(2)*, 779–89.

20. Romina, M., Gastón, L., Belén, R., Susana, R., Verónica, M., Fabricio, C. Evaluation of growth and motility in non-photosynthetic *Azospirillum brasilense* exposed to red, blue, and white light. Archives of Microbiology, 2020; 202:1193–1201.
21. Machado, H.B., Funayama, S., Rigo, L.U., Pedrosa, F.O. Excretion of ammonium by *Azospirillum brasilense* mutants resistant to ethylenediamine. *Can J Microbiol*. **1991**, *37(7)*, 549–53.
22. Santos, A.R.S., Etto, R.M., Furmam, R.W., Freitas, D.L. de Santos, K.F., d'Eça, N., de Souza, E.M., Pedrosa, F.O., Ayub, R.A., Steffens, M.B.R., Galvão, C.W. Labeled *Azospirillum brasilense* wild type and excretion-ammonium strains in association with barley roots. *Plant Physiology and Biochemistry*. **2017**, *118*, 422–426.
23. Näsvall, J., Knöppel, A., Andersson, D.I. Duplication-Insertion Recombineering: a fast and scar-free method for efficient transfer of multiple mutations in bacteria. *Nucleic Acids Res*. **2017**, *45(5)*, e3.
24. Pedrosa, F.O., Yates, M.G. Regulation of nitrogen fixation (nif) genes of *Azospirillum brasilense* by nifA and ntr (gln) type gene products. *FEMS Microbiology Letters*. **1984**, *23(1)*, 95–101.
25. Mempin, R., Tran, H., Chen, C., Gong, H., Ho, K.K., Lu S. Release of extracellular ATP by bacteria during growth. *BMC Microbiology*. **2013**, *13*, 301-314.
26. Yang, N.-C., Ho, W.-M., Chen Y.-H., Hu M.-L. A convenient one-step extraction of cellular ATP using boiling water for the Luciferin-Luciferase assay of ATP. *Anal. Biochem*. **2003**, *306*, 323-327.
27. Ehmann, A. The van URK-Salkowski reagent — a sensitive and specific chromogenic reagent for silica gel thin-layer chromatographic detection and identification of indole derivatives. *J Chromatography*. **1977**, *A132*, 267–276.
28. Park, S., Kim, A.-L., Hong Y.-K., Shin, J.-H., Joo, S.-H. A highly efficient auxin-producing bacterial strain and its effect on plant growth. *J Genet Eng Biotechnol*. **2021**, *19*, 179-188.
29. Graves, S.A., Hernandez, R., Fonslet, J., England, C.G., Valdovinos, H.F., Ellison, P.A., Barnhart, T.E., Elema, D.R., Theuer, C.P., Cai, W., Nickles, R.J., Severin, G.W. Novel preparation methods of Mn-52 for immunoPET imaging. *Bioconjugate Chemistry*. **2015,** *26(10)*, 2118–2124.
30. Inomura, K., Deutsch, C., Wilson, S.T., Masuda, T., Lawrenz, E., Bučinská, L., Sobotka, R., Gauglitz, J.M., Saito, M.A., Prášil, O., Follows, M.J. Quantifying oxygen management and temperature and light dependencies of nitrogen fixation by *Crocosphaera watsonii*. *mSphere*. **2019**, *4*, e00531-19.
31. Fixen, K.R., Zheng, Y., Harris, D.F., Shaw, S., Yang, Z.Y., Dean, D.R., Seefeldt, L.C., Harwood, C.S. Light-driven carbon dioxide reduction to methane by nitrogenase in a photosynthetic bacterium. *Proc Nat'l Acad Sci*. (USA) **2016**, *113(36)*, 10163–10167.
32. Zhang, Y., Burris, R.H., Ludden, P.W., Roberts, G.P. Regulation of nitrogen fixation in *Azospirillum brasilense*. *FEMS Microbiol Lett*. **1997**, *152(2)*, 195–204.
33. Vekshin, N.L. Light-dependent ATP synthesis in mitochondria. *Biochem Int*. **1991**, *25(4)*, 603-611.
34. Fu, H.A., Hartmann, A., Lowery R.G., Fitzmaurice W.P., Roberts G.P., Burris R.H. Posttranslational regulatory system for nitrogenase activity in *Azospirillum* spp. *J Bacteriol*. **1989**, *171*, 4679-4685.
35. Klassen, G., de Souza, E.M., Yates, M.G., Rigo, L.U., Inaba, J., Pedrosa, F.O. Control of nitrogenase reactivation by the GlnZ protein in *Azospirillum brasilense*. *J. Bacteriol*. **2001**, *183*, 6710-6713.
36. Huergo, L.F., Chubatsu, L.S., de Souza, E.M., Pedrosa, F.O., Steffens M.B.R, Merrick, M. Interactions between P_{II} proteins and the nitrogenase regulatory enzymes DraT and DraG in *Azospirillum brasilense*. *FEBS Letters*. **2006**, *580(12)*, 5232-5236.
37. Wenke, B.B., Spatzal, T., Rees, D.C. Site-specific oxidation state assignments of the iron atoms in the $[4Fe:4S]^{2+/1+/0}$ states of the nitrogenase Fe-protein. *Angewandte Chemie. International Edition*. **2019**, *58(12)*, 3894–3897.
38. Woodward, A.W., Bartel, B. Auxin: regulation, action, and interaction. *Ann Bot*. **2005**, *95*, 707–735.
39. McSteen, P. Auxin and monocot development. Cold Spring Harbor Perspective Biol. **2010**, *2(3)*, a001479.
40. Agtuca, B., Rieger, E., Hilger, K., Song, L., Robert, C.A.M., Erb, M., Karve, A., Ferrieri, R.A. Carbon-11 reveals opposing roles of auxin and salicylate in regulating leaf physiology, leaf metabolism and resource allocation patterns that impact root growth in *Zea mays*. *J Plant Growth Regulation*. **2014**, *33(2)*, 328-339.
41. Schmid, J., Amrhein, N. Molecular organization of the shikimate pathway in higher plants. *Phytochemistry*. **1995**, *39*, 737-749.
42. Bender, S.L., Mehdi, S., Knowles, J.R. Dehydroquinate synthase: The role of divalent metal cations and of nicotinamide adenine dinucleotide in catalysis. *Biochemistry*. **1989**, *28*, 7555-7560.
43. Schneider, D.A., Gourse, R.L. Relationship between growth rate and ATP concentration in *Eschericha coli*. *J Biological Chemistry*. **2004**, *279(9)*, 8262-8268.